A&A 384, 812–825 (2002)
DOI: 10.1051/0004-6361:20020110

Astronomy & Astrophysics

1.65 μm (H-band) surface photometry of galaxies

IX. Photometric and structural properties of galaxies

M. Scodeggio[1], G. Gavazzi[2], P. Franzetti[1,2], A. Boselli[3], S. Zibetti[2], and D. Pierini[4]

[1] Istituto di Fisica Cosmica "G. Occhialini", CNR, via Bassini 15, 20133, Milano, Italy
[2] Università degli Studi di Milano – Bicocca, P.zza dell'Ateneo Nuovo 1, 20126 Milano, Italy
[3] Laboratoire d'Astrophysique de Marseille, Traverse du Siphon, 13376 Marseille Cedex 12, France
[4] Dept. of Physics and Astronomy, University of Toledo, 2801 W. Bancroft, 43606, Toledo, Ohio, USA

Received 31 July 2001 / Accepted 8 January 2002

Abstract. As a result of a systematic NIR H-band (1.65 μm) imaging survey of normal galaxies in the local universe that includes objects both in the Virgo cluster and in the "Great Wall" (including A1367, A1656 as well as the "isolated" population in the bridge between the two clusters), we are able to measure in a highly homogeneous way photometric and structural properties for a sample of 1143 galaxies. We base our analysis on a quantitative structural parameter, the concentration index C_{31} (defined as the ratio between the radii that enclose 75% and 25% of the total luminosity), instead of relying on the galaxies' morphological classification. The C_{31} parameter provides a model independent, quantitative and continuous characterization of the light distribution within galaxies, and it is thus to be preferred to either the Hubble type or a parameter like the bulge-to-disk or bulge-to-total light ratio. Low C_{31} objects are typically found among disk galaxies, while high C_{31} describes bulge-dominated systems. We confirm our previous claim that C_{31} correlates strongly and non-linearly with the galaxy total luminosity. $C_{31} > 5$ values are found only at $L_H > 10^{10}\ L_\odot$ (giant ellipticals mixed with early-type spirals), while at $L_H < 10^{10}\ L_\odot$ galaxies have $C_{31} < 3$ (dwarf Irregulars mixed with ellipticals). At high luminosity, low C_{31} are allowed (bulge-less giant Scs). Thus C_{31} and the total luminosity are not sufficient to fully characterize the family of galaxies. However we find that galaxies can be completely described by three parameters, namely: a scale parameter (the H-band luminosity), a shape parameter (the concentration index C_{31}) and a colour parameter (e.g. the $B-H$ colour). At low luminosity dEs and dIs, having similar C_{31}, are colour-discriminated, while at very high luminosity different C_{31} discriminate S0s from Scs, otherwise undistinguishable on the basis of their colour. A single, monotonic relation exists between luminosity and μ_e in the H-band, as opposed to the two separate regimes that are generally observed in the B-band. As NIR luminosity traces quite accurately the galaxy mass distribution, this relation re-enforces the indication in favour of a scale-dependent mass collapse mechanism which produces higher surface-brightness and more centrally peaked galaxies with increasing mass. However, the presence of high-luminosity low-C_{31} galaxies hints at other machanisms and physical properties (such as angular momentum) playing an important role in galaxy formation.

Key words. galaxies: fundamental parameters – galaxies: photometry – infrared: galaxies

1. Introduction

The most commonly used galaxy classification system is the one originally developed by Hubble (1936), and brought to completion by Sandage (1961). Among the main reasons for its success are the fact that it is relatively easy to use, and the fact that it has proven successful in ordering the "realm of nebulae" according to important physical characteristics. The correlations between quantities related to a galaxy stellar population (like galaxy color) and Hubble type are well known (see Roberts & Haynes 1994 for a recent review). However, the Hubble classification system suffers from a number of important drawbacks that are becoming more and more evident as the samples of galaxies studied in detail become larger both at low and high redshift. Among these drawbacks, its qualitative and quantized nature, that prevents fitting relations as a function of type on a solid statistical basis, and the fact that a large (and ever-growing, with the completion of new surveys) fraction of galaxies cannot fit well inside the scheme, are the most limiting features.

These and other limitations of the Hubble system have been recognized for a long time, and a number of extensions to the scheme, or alternative classification

Send offprint requests to: M. Scodeggio,
e-mail: marcos@ifctr.mi.cnr.it

schemes, have been proposed through the years. Best-known among such efforts are the extension to the Hubble system devised by de Vaucouleurs (1959), and the alternative scheme proposed by Morgan (1958, 1959). Still, neither of these schemes is widely used by the astronomical community. More recently, Whitmore (1984) proposed a sound, quantitative scheme for the classification of spiral galaxies, that is based on two parameters: "scale" and "form" (following Whitmore's terminology). The scale parameter is a combination of the galaxy absolute blue luminosity and isophotal radius, while the form is a combination of the galaxy color and bulge-to-total light ratio. This idea has been further developed by Bershady et al. (2000; hereafter BJC), who have presented a classification scheme encompassing all morphological types. In doing so, they were forced to increase the dimensionality of the classification volume from two to three dimensions, that they define to be a spectral index (galaxy color), a scale (galaxy surface brightness), and a form (galaxy light concentration, or asymmetry) parameter. This classification scheme is fully quantitative, can be used to classify galaxies over a broad range of redshifts (provided that images with enough spatial resolution can be obtained), and is quite successful in separating normal galaxies into classes that are largely coincident with those one would obtain using Hubble types.

One important feature for a classification scheme should be its ability to describe not only the "current" status of a galaxy (by "current" we mean the status at the epoch of the observation, the latter being of course dependent on the galaxy redshift), but also its evolutionary history. This goal however is complicated by the degeneracy that many galaxy parameters show with respect to different possible formation and evolution histories. A well-known example is the age-metallicity degeneracy for stellar populations in early-type galaxies (Worthey 1994), but we observe a rather similar color-star formation history degeneracy for late-type, star-forming galaxies (Gavazzi et al. 2002). To achieve the goal of obtaining a classification scheme that might provide information on a galaxy's past evolutionary history we are building a large dataset of multifrequency observations of nearby galaxies, that covers objects of all morphological types over an extended range of luminosities and environmental conditions, from the cores of dense clusters to relatively under-dense regions in the field. We began our effort by focusing on late-type star-forming galaxies, and the results of the analysis of these systems are summarized in Gavazzi et al. (1996c), and Gavazzi & Scodeggio (1996). Since then we have extended our sample to also cover early-type galaxies, and we have completed a photometric near-infrared (H-band) imaging survey that covers a large fraction of our total sample, to measure in a completely homogeneous fashion the photometric and structural properties of nearby normal galaxies. Previous papers in this series describe the photometric survey (Gavazzi et al. 1996a – Paper I; Gavazzi et al. 1996b – Paper II; Boselli et al. 1997; Gavazzi et al. 2000a – Paper III; Boselli et al. 2000 – Paper IV; Gavazzi et al. 2001 – Paper VII) and provide details on the derivation of the photometric parameters used here (Gavazzi et al. 2000b – Paper V). In this work we describe the observed correlations between photometric and structural properties for the galaxies in our sample. For the first time this kind of analysis is presented using H-band near-infrared imaging data. This offers two key advantages with respect to the more often used optical bands imaging: a much smaller influence from dust extinction on the observed parameters, and the capability of tracing the bulk of the luminous matter mass, without being heavily influenced by the small fraction of young stars that often dominate galaxy emission in the blue optical bands. Two other papers in this series discuss the correlation between their photometric, structural, and dynamical properties (Pierini et al. 2002), and the correlation between these properties and the galaxy star formation history (Boselli et al. 2001). A future paper will discuss the practical application of our classification scheme to a sample of more distant galaxies.

2. The data

The analysis of photometric and structural properties of normal galaxies we carry out in this paper is based on a nearly complete Near Infrared H-band survey of an optically selected sample of nearby galaxies. Full details about the sample selection, the observations, and the data reduction procedures can be found in the previous papers of this series (Papers I, II, III, IV, VII), and here only a brief summary is presented.

Our sample includes all galaxies from the CGCG catalogue (Zwicky et al. 1961–1968) ($m_{\rm pg} \leq 15.7$) that belong to the Coma supercluster region, including the two clusters Coma (A1656) and A1367, and to the clusters A262 and Cancer, and galaxies from the VCC catalogue (Binggeli et al. 1985) (restricted to $m_{\rm pg} \leq 16.0$) in the Virgo cluster. Observations were carried out from 1993 to 1997 with the 1.5 m TIRGO and with the Calar Alto 2.2 and 3.5 m telescopes equipped with the NICMOS3 256^2 pixel arrays cameras ARNICA and MAGIC, respectively, and more recently with the ESO NTT and TNG telescopes, equipped with the SOFI and NICS or ARNICA cameras. In total we have obtained observations for 1302 galaxies, that span all morphological types from E and dE to dIrr. However, because of the selection criterion of our master catalog, extremely low surface brightness galaxies are not included in our sample. Paper VII provides information on the completeness of our observations.

The surface photometry measurements used in this paper are discussed in detail in Paper V. Each galaxy two-dimensional light distribution was fitted with elliptical isophotes to derive a radial surface brightness profile. This profile was fitted with either a de Vaucouleurs $r^{1/4}$ or an exponential disk profile, or a combination of two profiles (either a de Vaucouleurs plus exponential disk, or two exponential profiles, the choice being based on a

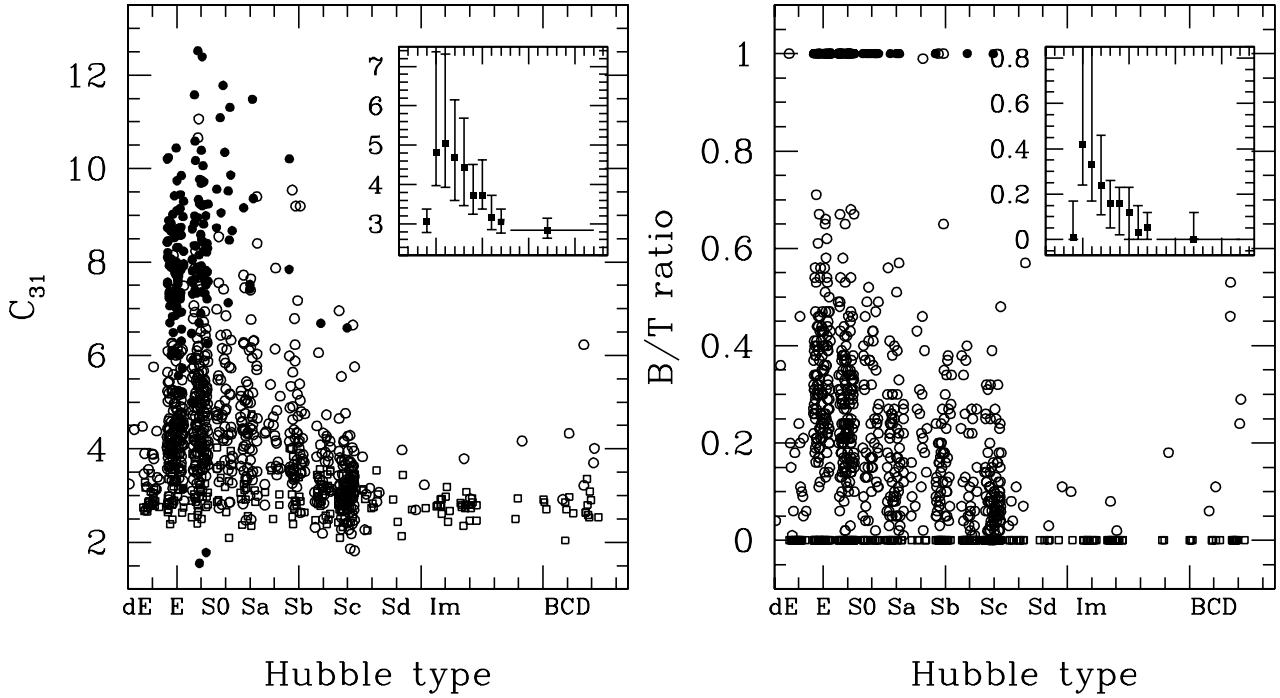

Fig. 1. The distribution of concentration index C_{31} values (left panel), and of bulge to total light ratio B/T values (right panel), as a function of Hubble type. Filled circles represent galaxies with a pure de Vaucouleurs radial profile, empty squares galaxies with a pure exponential disk profile, and empty circles galaxies with a composite profile. To make the density of data points more readily visible, we offset the abscissa of each point in the graph by a small, random amount. The insets show the median C_{31} and B/T value for each type (filled squares), and the upper and lower quartiles of their distributions. Types later than Sc are grouped together to improve statistics.

best fit criterion). Among the 1302 profiles, 192 are fitted with a pure de Vaucouleurs $r^{1/4}$ law and 369 with a pure exponential one. The remaining profiles require a Bulge+Disk (B+D) decomposition, with 54 objects showing signs of a truncated outer light distribution. We have also tried to fit the global surface brightness profile with a single Sérsic (1968) $r^{1/n}$ profile, but we could not reproduce at all the shape of the observed profile for a large fraction of the B+D galaxies, and therefore abandoned this experiment. A total magnitude $H_{\rm T}$ was derived for each galaxy by extrapolating the suitable profile to infinity, and adding the extrapolated light contribution to the one measured within the last fitted isophote. Empirical effective radius $r_{\rm e}$ (the radius within which is contained half of the galaxy light) and effective surface brightness $\mu_{\rm e}$ (the mean surface brightness within the effective radius) were measured on the observed profile, at the half light point, on the basis of the total magnitude determination. Bulge and disk parameters were derived from the fitted profiles, together with the bulge to total (B/T) light flux (the ratio of the bulge flux to the total flux from the galaxy). We also derived for each galaxy an isophotal radius $r_H(20.5)$ determined in the elliptical azimuthally–integrated profiles as the radius at which the surface brightness reaches 20.5 H–mag arcsec^{-2}, and a concentration index (C_{31}), defined as in de Vaucouleurs (1977) to be the model–independent ratio between the radii that enclose 75% and 25% of the total light $H_{\rm T}$. The median uncertainty in the

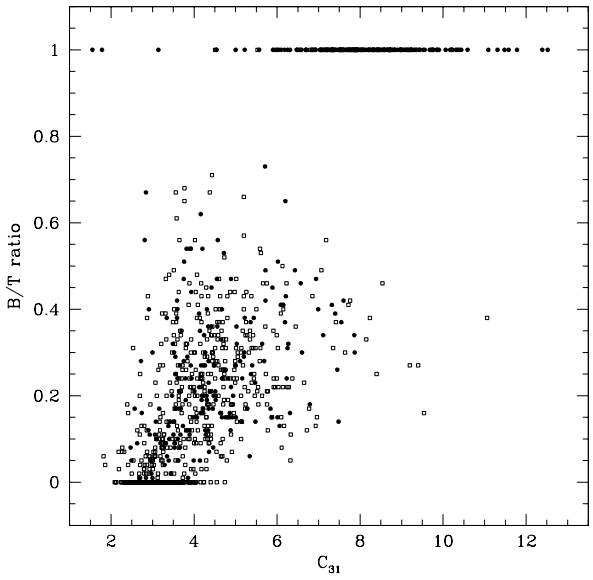

Fig. 2. The relation between the concentration index C_{31} and the bulge-to-total light ratio for the galaxies in our sample. Same symbols as in the previous figures.

determination of the total magnitude is 0.15 mag, while those on the determination of log $r_{\rm e}$ and $\mu_{\rm e}$ are 0.05 and 0.16 mag, respectively.

Although we do not use Hubble types as a basis for the classification of galaxies, we have tried to leave the

possibility of a comparison with the traditional classification scheme open. For this reason in the following analysis we exclude from our sample a number of galaxies that have very uncertain morphological classification (90), and peculiar galaxies (69). The total sample used here is therefore composed of 1143 galaxies. Of these, 831 have color measurements available, and are used in the definition of our classification scheme (see Sect. 4).

3. The concentration index

A concentration index has been used before as a classification tool, most noticeably in the Morgan classification scheme (Morgan 1958, 1959). Other classification schemes involving a concentration index have been proposed, usually trying to take advantage of the correlation existing between image concentration and mean surface brightness in galaxies (e.g. Okamura et al. 1984; Kent 1985; Doi et al. 1993; Abraham et al. 1994). Most recently BJC have presented a global classification scheme for galaxies that includes a concentration index as one of the fundamental classification parameters, along with color, surface brightness, and galaxy asymmetry. All their parameters were derived from B-band imaging data. They find correlations to be present between concentration and either color, surface brightness, or asymmetry, the strongest one being that between concentration and color.

Here we adopt a definition of concentration index which is somewhat different from the one used by BJC. We define, following de Vaucouleurs (1977), the concentration index C_{31} as the ratio between the radii that enclose 75% and 25% of the total galaxy light $H_{\rm T}$, whereas BJC take the logarithm of the ratio between two radii (specifically, those that enclose 80% and 20% of the total light). As we discuss in Sect. 4, we consider our "linear ratio" definition better suited to emphasize the changes of fundamental galaxy properties as a function of galaxy luminosity, as discussed already in Gavazzi et al. (1996c). With our definition of concentration index, a pure de Vaucouleurs profile should have $C_{31} = 7.02$, while a pure exponential disk profile should have $C_{31} = 2.80$.

It is quite natural to expect a correlation between the value of C_{31} and other parameters traditionally used for galaxy classification, like Hubble type, or bulge-to-disk/bulge-to-total light ratios, as the relevance of the bulge inside a galaxy is one of the main parameters in the Hubble scheme, and the only reliable one for edge-on spiral galaxies. We show in the left panel of Fig. 1 the distribution of C_{31} values as a function of Hubble type. Two characteristics are clearly evident: there is a general correlation between C_{31} and type, as evidenced by the global decline in the median C_{31} value going from ellipticals to late type spirals (with dE galaxies representing an exception with respect to this trend; see the figure inset), but there is also a large scatter within a given type, at least up to type Sb. Part of this scatter might result from misclassifications, due to the greater difficulty in classifying galaxies at the distance of the Coma supercluster with respect to those in the Virgo cluster, but a component of this scatter is due to a real dependence of C_{31} on galaxy luminosity, as discussed in Sect. 4. It is therefore clear that concentration index and Hubble type are not completely equivalent classification criteria.

The same situation is present when considering the B/T light ratio. As shown in the right panel of Fig. 1 there exists also for B/T a global correlation with Hubble type, with a decline in the median value of B/T when going from ellipticals to late type spirals, and a large scatter within each Hubble type. Also in this case there are classification problems and a real dependence of the B/T ratio on galaxy luminosity that contributes to the scatter. Therefore also the B/T ratio is not a classification criterion equivalent to Hubble type, and it is not equivalent either to the concentration index criterion, as shown in Fig. 2, where we see the presence of a rather large scatter in the value of B/T for any given value of C_{31}.

Keeping in mind these differences, and the fact that all three form criteria (Hubble type, concentration index, and B/T ratio) share some common basis in terms of their ability to differentiate among galaxies with different appearance, structure, and stellar populations, we choose to base our "form" classification on the concentration index C_{31}. With respect to Hubble type it has the advantage of being a quantitative index, that can be easily measured for all galaxies independently from the observer's viewing angle, and is less affected by distance related resolution problems. With respect to the B/T ratio, it has the advantage of being model independent, not requiring the decomposition of a galaxy into a bulge and a disk component, a process which is always affected by considerable uncertainties. Another advantage offered by the concentration index is its continuous distribution of values, as compared to the quantized distribution of Hubble types, and the peculiar distribution of B/T values (composite B+D photometric profiles show a continuous distribution of values, but pure de Vaucouleurs profiles have B/T equal to 1, and pure exponential disk profiles have B/T equal to 0 by definition).

Finally we remark that, at least in the H-band, where internal dust extinction effects are quite negligible, galaxy viewing angle has little influence on the derivation of C_{31} values. The distribution of C_{31} covers the full range of observed values at all galaxy inclinations (as derived from the observed axial ratio), but we observe a moderately significant trend toward higher C_{31} values at high inclination. The median C_{31} value for galaxies with inclination below 50 degrees is 2.99, while for galaxies with higher inclination is 3.56 (in both cases the distribution has a standard deviation of approximately 1.5).

4. Scale, form, and color

Whitmore (1984) introduced the first quantitative galaxy classification scheme that incorporates both structural and spectral parameters, introducing the concepts of galaxy "scale" (in his analysis a combination of absolute

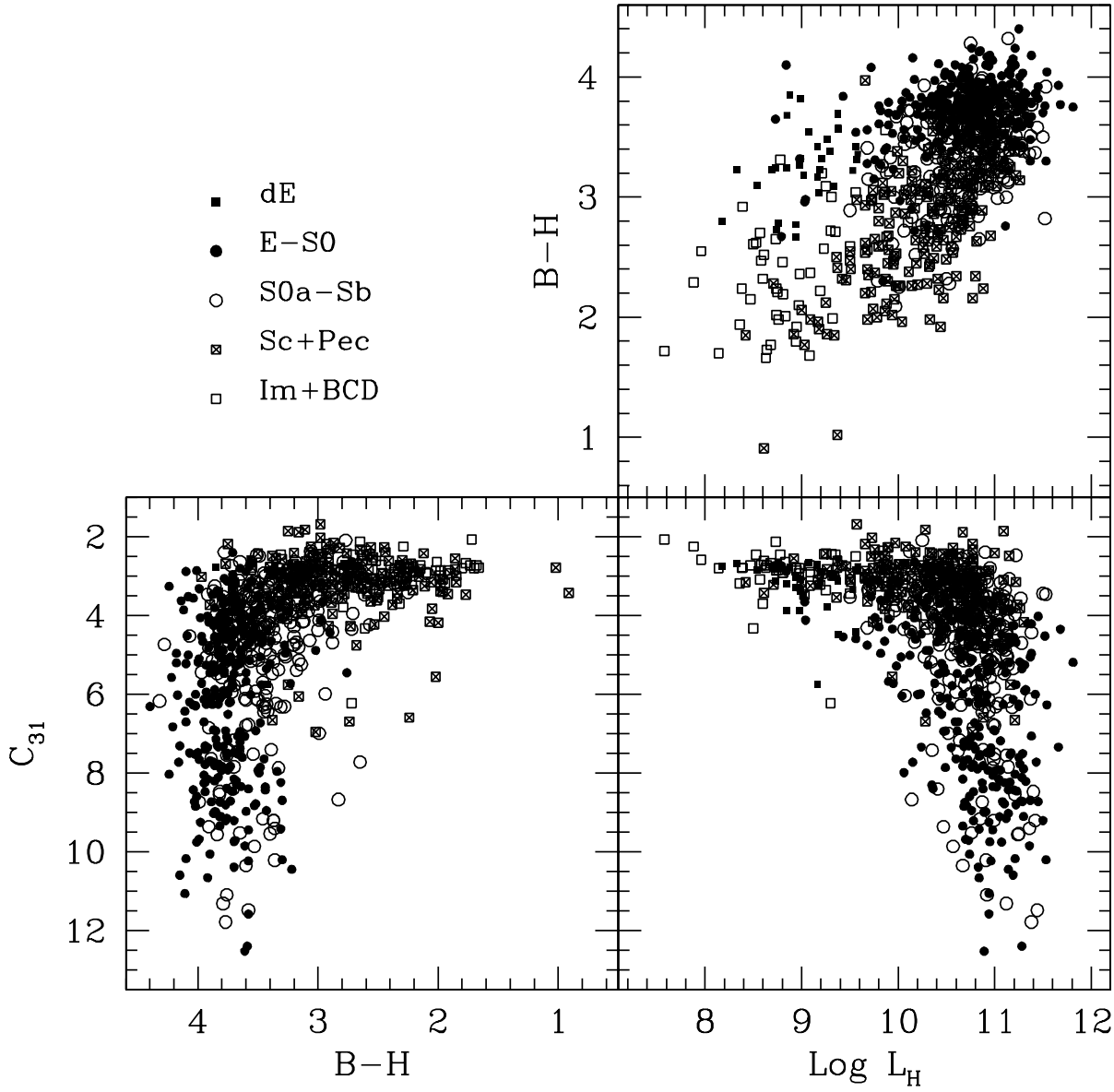

Fig. 3. The distribution of H-band luminosity L_H, $B-H$ color, and concentration index C_{31} for the galaxies in our sample. Different symbols identify galaxies within different ranges of Hubble types, as detailed in the legend.

blue luminosity and isophotal radius) and "form" (in his analysis a combination of $B-H$ color and B/T light ratio). He concluded that these two parameters would provide an optimal classification scheme for spiral galaxies, to which his work was limited. His choice for the specific combinations that define the form and scale parameters was based on the observation that those quantities show the strongest correlations between themselves among the 30 parameters taken into consideration in his work. More recently BJC have presented a quantitative classification scheme along the same lines, extended to galaxies of all morphological types. However they need three parameters to obtain a satisfactory classification of all galaxies: a spectral index ($B-V$ color), a scale (surface brightness), and a form (concentration index or image asymmetry) parameter.

4.1. The luminosity, color, C_{31} cube

Independently from BJC, we have defined a very similar framework to describe the main structural and photometric properties of normal galaxies. Our sample in fact does not include a significant fraction of starbursting, interacting, or extremely low surface brightness objects. In agreement with BJC, we conclude that at least three parameters are needed to provide a unique classification for all galaxies. Figures 3 and 6 show two alternatives definitions for such a classification cube. The first one, presented in Fig. 3 is based on H-band luminosity, color (either $B-H$ or $B-V$, this second not shown in the figure), and concentration index C_{31}. In the second one, presented in Fig. 6, the effective surface brightness μ_e replaces the H-band luminosity. To keep the connection with the Hubble types

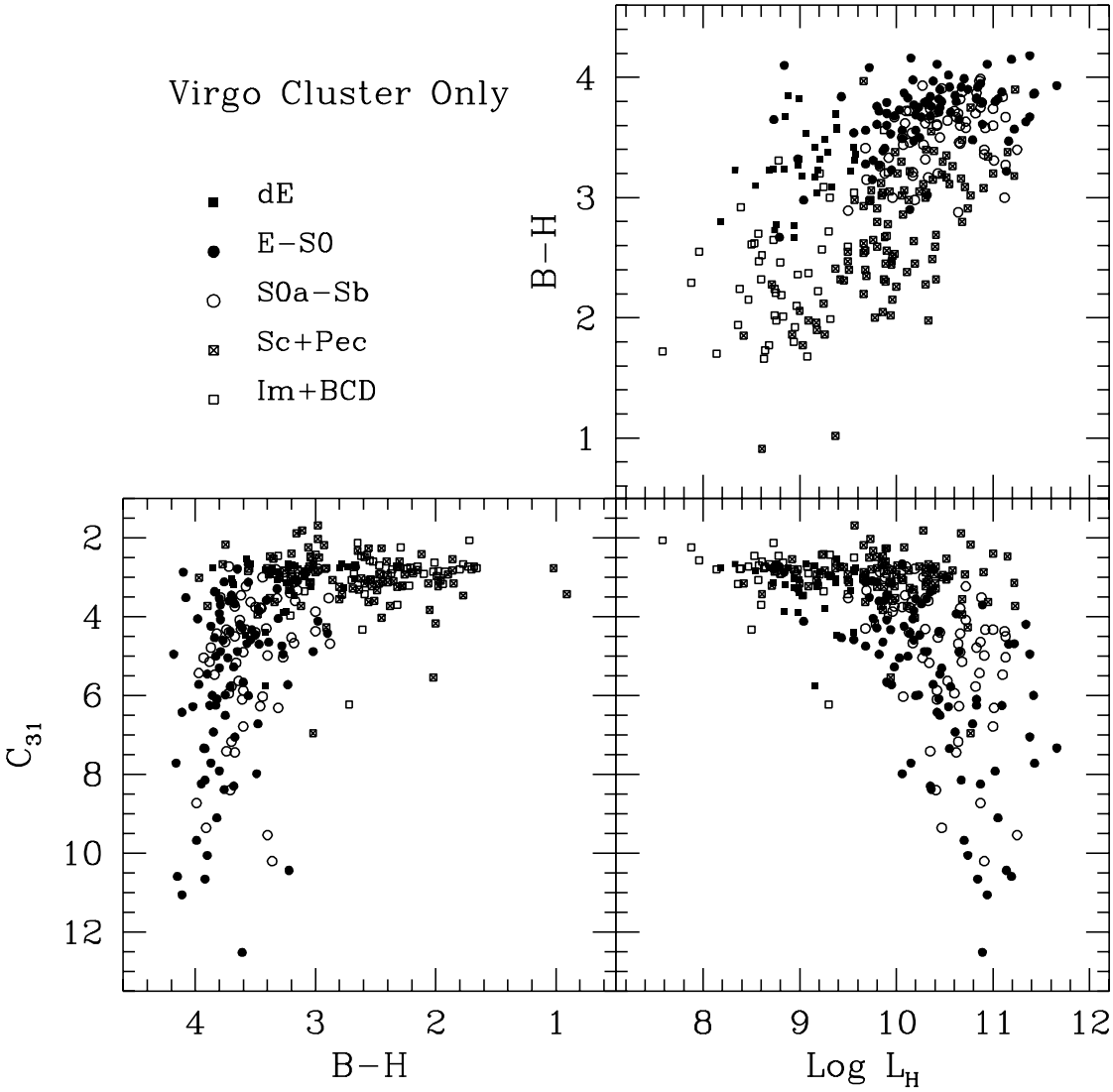

Fig. 4. The distribution of H-band luminosity L_H, $B-H$ color, and concentration index C_{31} as in the previous figure, but limited to Virgo Cluster galaxies only.

classification open, in both figures different symbols identify galaxies within different ranges of Hubble types.

It is well known that both early- and late-type galaxies obey a color-luminosity relation (see, for example, Visvanathan & Sandage 1977; Bower et al. 1992 for early-type galaxies, and Tully et al. 1982; Gavazzi et al. 1996c for spiral galaxies). Since the two relations are quite different, their origins are also believed to be different. The small color changes of early-type galaxies are most likely produced by metallicity variations within a coeval galaxy population (Arimoto & Yoshii 1987; see however Worthey et al. 1996 for a discussion on the effects of age variations within a metal homogeneous population). The much broader color range covered by late-type galaxies is mainly the result of a broad range of star formation histories (Searle et al. 1973; Kennicutt 1983; Sandage 1986), coupled with an equally broad range of dust extinction values. This color-luminosity correlation is well visible in the upper panel of Fig. 3.

BJC have also already described a correlation between color and B-band concentration index, although they did not discuss what we consider to be the main feature visible in the lower panels of Figs. 3 and 6, which is the strong non-linearity in the correlation between C_{31} and either color, H-band luminosity, or effective surface brightness. It is clearly evident from these figures that there are two main regimes of galaxy properties, that produce two almost orthogonal distributions in the parameter space we are considering. At low luminosity ($L_H < 10^{10}\ L_\odot$) all galaxies consistently have very small C_{31}, independently from their color (and from their Hubble type, for that matter), while only at high luminosity ($L_H > 10^{10}\ L_\odot$) we observe galaxies with large values of C_{31}. At the same time blue galaxies consistently have low values of C_{31}, and it is only among the red ones that large values of C_{31} are present. Alternatively, we can say that galaxies with small C_{31} can have all colors and all luminosities, while those with a large C_{31} are only found among red luminous

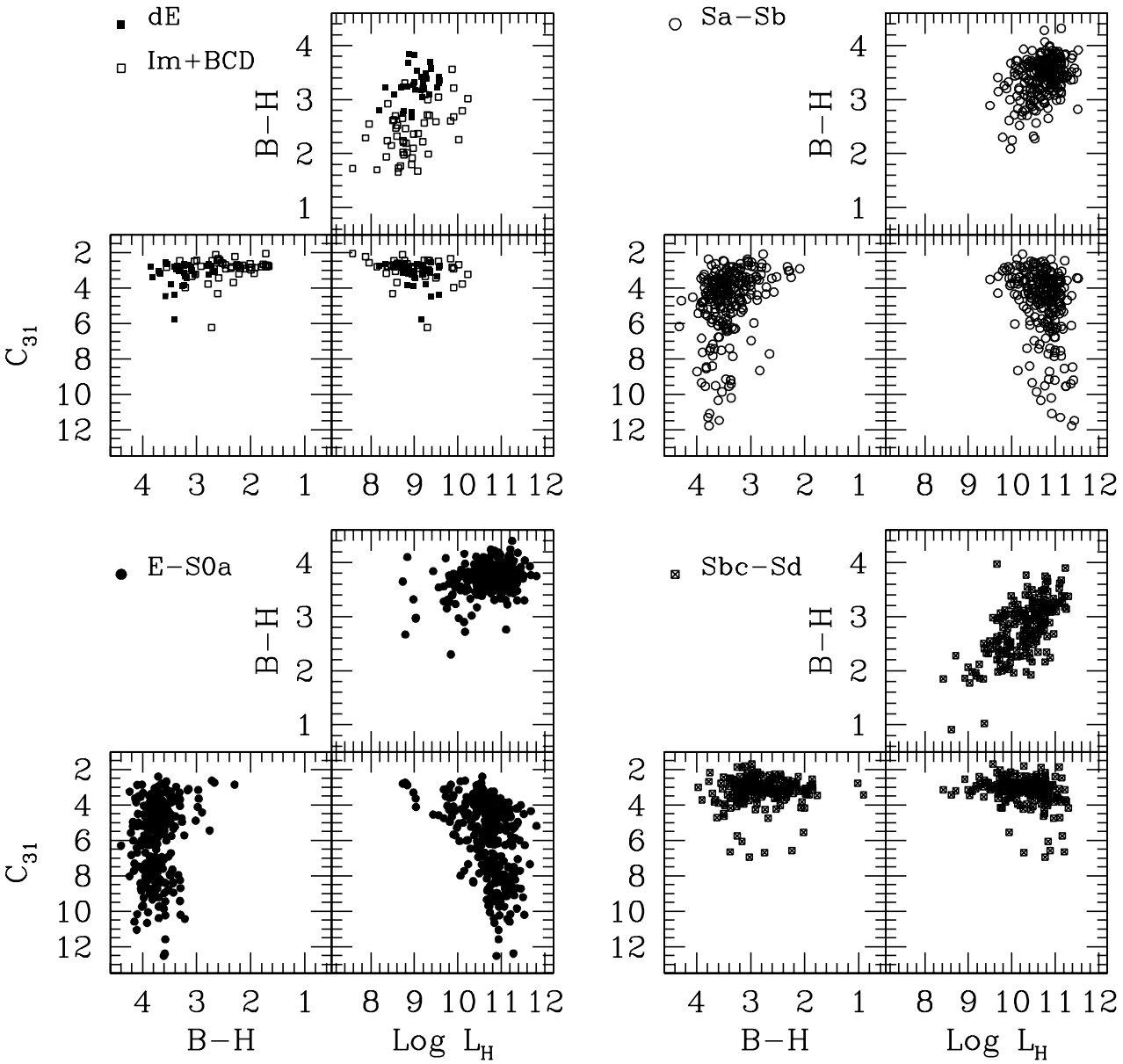

Fig. 5. The distribution of H-band luminosity L_H, $B-H$ color, and concentration index C_{31} for the galaxies in our sample, divided into 4 groups of morphological types. In the left half of the plot we present dwarf galaxies (both dE and dIrr) on the top part and E plus S0 galaxies on the bottom part. In the right half of the plot we present Sa and Sb galaxies on the top part, and Sc and Sd galaxies on the bottom part.

objects. We stress here the fact that this qualitative picture is not sensitive to the choice of photometric bands used to derive the color parameter, at least as far as optical or optical-near infrared colors are involved. The finding of a luminosity threshold for the appearance of high C_{31} values is in agreement with the finding discussed in Papers V and VII, that pure de Vaucouleurs profiles are absent from the classification of photometric profiles below the luminosity $L_H \simeq 10^{10}\ L_\odot$.

As discussed in Sect. 2 our sample is composed mainly of galaxies from the Coma Supercluster and the Virgo Cluster. The different distance of these two structures translates into different completeness limits when luminosity is taken into consideration. To provide a more reliable indication of the relative density of galaxies in the various parts of our classification cube we reproduce it again in Fig. 4, plotting in this case only Virgo Cluster galaxies. Notice that even in this case, however, for luminosities $L_H < 10^9\ L_\odot$ sample incompleteness becomes non-negligible, and the density of galaxies in the plot does not represent any more the true fraction of objects that lay in this part of the galaxies' parameter space. The most striking difference between Figs. 3 and 4 concerns spiral galaxies. Within the global sample the color-magnitude relation for these objects appears much steeper than in the more complete Virgo sample, purely as a result of sample incompleteness. In fact our sample is an optically selected one, complete down to a certain optical magnitude

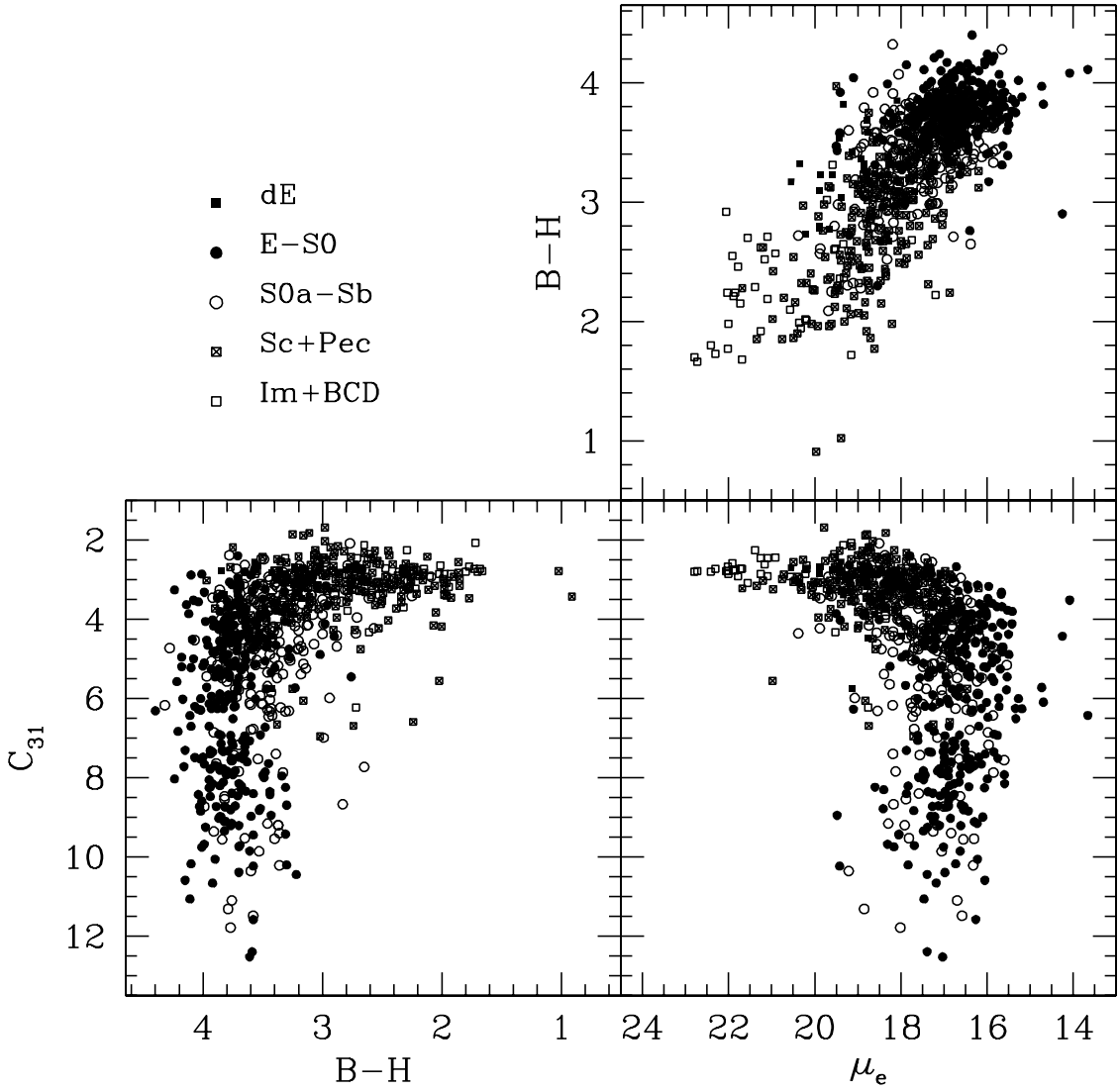

Fig. 6. The distribution of effective surface brightness μ_e, $B-V$ color, and concentration index C_{31} for the galaxies in our sample. As in the previous figure, different symbols identify galaxies within different ranges of Hubble types.

(as discussed in Sect. 2). Therefore when one considers H-band data, the magnitude limit for the sample changes with galaxy color, shifting to brighter luminosities as the color changes from blue to red (a diagonal line in Fig. 3).

To better illustrate the relation between the classification cube presented here and the classic Hubble classification scheme, we present in Fig. 5 the same plots as in Fig. 3, separating the galaxies in different panels according to their Hubble type. It is evident from these figures that the scatter within the C_{31}-Hubble type relation can be partly explained by the luminosity (color) dependence of the concentration index, that is quite evident even when a restricted range of Hubble types is considered.

4.2. The μ_e, color, C_{31} cube

An almost equivalent picture to that presented in Fig. 3 is obtained substituting the effective surface brightness μ_e to the H-band luminosity (see Fig. 6). There are nonetheless two noticeable differences between these two data cubes. The first one is the smaller scatter shown by the μ_e-color relation with respect to the luminosity-color one. This results mainly from a lack of low μ_e ellipticals, while late-type galaxies show similar behaviour in the two diagrams. This effect could however be due to an observational bias, as red objects with μ_e fainter than 20 H–mag arcsec^{-2} are very difficult to observe and detect in the near infrared. As a result our sample is strongly incomplete with respect to dwarf-elliptical galaxies. Should the smaller scatter be confirmed even after the completion of our survey, it could probably be explained by the fact that μ_e is not purely a scale parameter like luminosity, but a hybrid one, mixing both scale and form in its definition. The second difference is the total absence of a correlation between μ_e and C_{31} for high C_{31} objects, compared to a small but significant trend between luminosity and C_{31} (the mean $\log L_H$ for objects with $4 < C_{31} < 5$ is 10.6, while for objects with $C_{31} > 9$ it is 11.0). Another interesting result is the fact

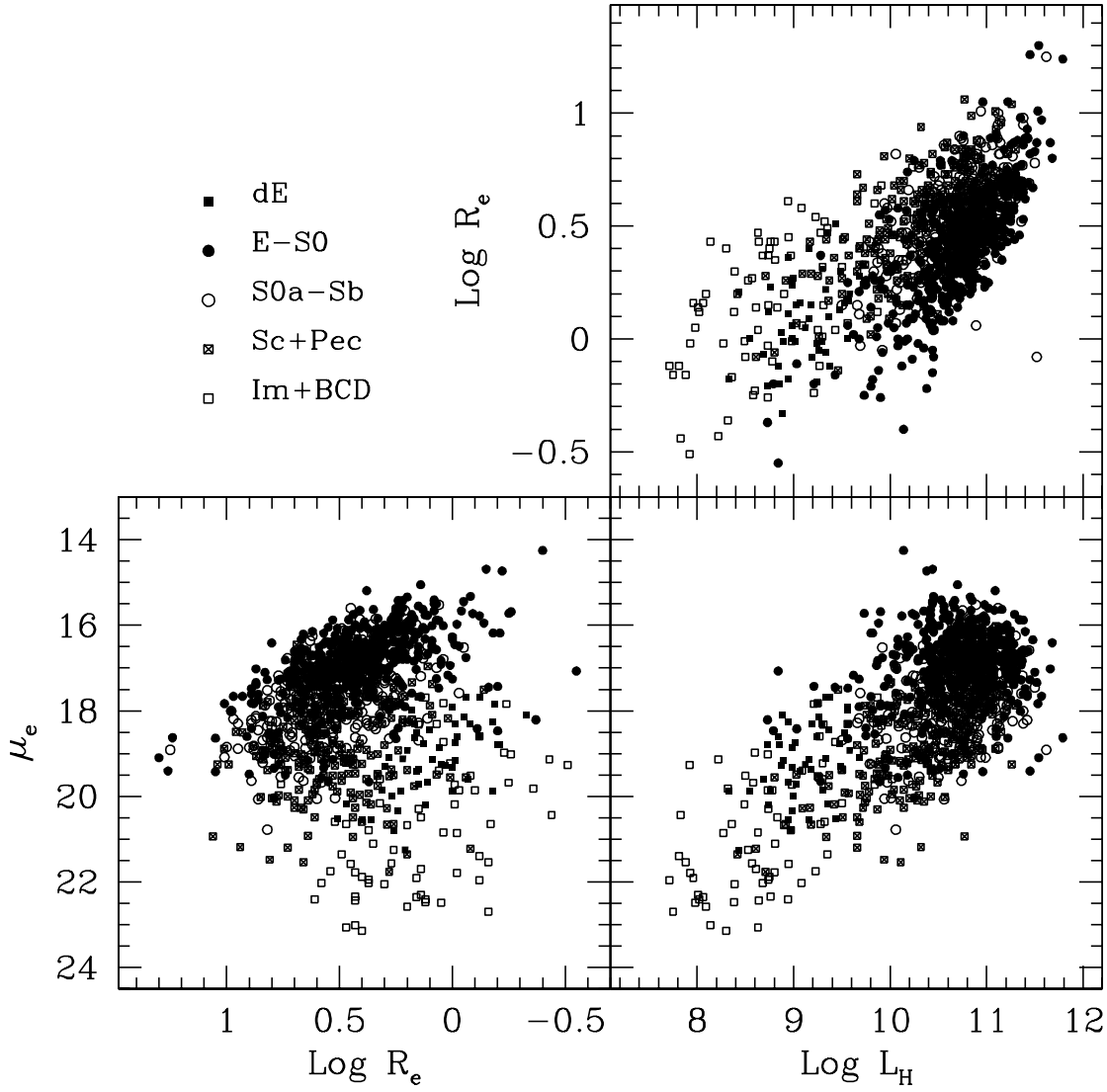

Fig. 7. The distribution of H-band luminosity L_H, effective surface brightness μ_e, and effective radius r_e for the galaxies in our sample. Different symbols identify galaxies within different ranges of Hubble types, as in the previous figures.

that the observed strong correlation between μ_e and color, which confirms earlier results presented by Gavazzi et al. (1996c), is in disagreement with the results presented by BJC (see the upper panels of their Fig. 3), that confirm instead the so-called Freeman's law (Freeman 1970). This is yet another indication that the validity of Freeman's law is limited to one specific photometric band.

It could be argued that this second classification cube is better suited than the one discussed in the previous section to represent normal galaxy properties, both because of the smaller scatter observed in the μ_e-color relation with respect to the L_H-color one (should this feature be confirmed when observations of our sample will be completed), and because surface brightness is a distance-independent quantity (cosmological dimming correction aside), whereas luminosity is not. However what could be better in terms of a classification scheme might not be equally relevant in building a physical model for galaxy formation and evolution. In that case total near infrared luminosity, which is a good tracer of galaxy mass, should be certainly considered as a more fundamental parameter than surface brightness.

5. The photometric fundamental plane

The possibility of replacing H-band luminosity with effective surface brightness in the classification cube, as discussed above, is due to the presence of a significant correlation between those two quantities. In fact a number of correlations are known to exist, at least for early-type galaxies, that involve luminosity, effective surface brightness, and effective radius. Luminosity correlates with effective radius (Fish 1964), stellar velocity dispersion (Faber & Jackson 1976), and effective surface brightness (Binggeli et al. 1984), while effective radius and effective surface brightness correlate among themselves (Kormendy 1977; see Guzmán et al. 1993 for a global discussion about these correlations). These relations exhibit a larger scatter than

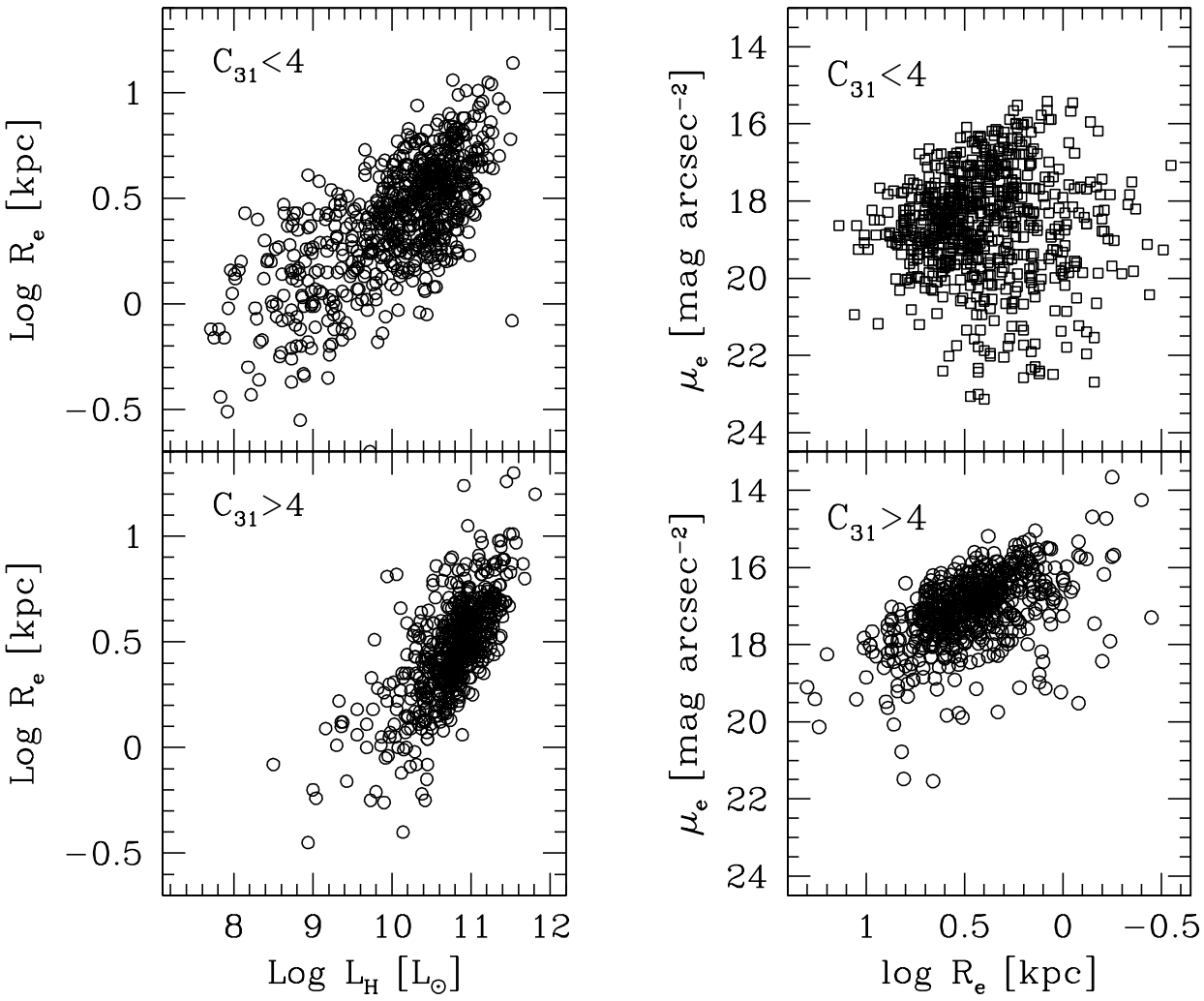

Fig. 8. The correlation between H-band luminosity L_H and effective radius r_e (left panels), and that between effective radius r_e and effective surface brightness μ_e (right panels) for the galaxies in our sample, divided into two groups according to their C_{31} values. The top panels shows galaxies with $C_{31} \leq 4$, while the bottom one shows those with $C_{31} > 4$.

can be accounted for by measurement errors alone, and this lead to the idea that early-type galaxies populate a plane in the 3–parameter space of effective radius, effective surface brightness and stellar velocity dispersion, independently introduced by Djorgovski & Davis (1987) and by Dressler et al. (1987). Modified versions of this Fundamental Plane relation have since then been proposed, that use color (de Carvalho & Djorgovski 1989) and luminosity (Scodeggio et al. 1997) as a substitute for the stellar velocity dispersion.

A Photometric Fundamental Plane correlating galaxy luminosity, effective radius r_e and effective surface brightness μ_e still exists[1] even when considering galaxies of all morphological types, as shown in Fig. 7. However, as it could be expected, the picture one obtains when considering galaxies of all types is more complex than the one provided by early-type objects alone. While the shape and scatter of the luminosity-μ_e relation are not influenced by the sample morphological mix, both the r_e-luminosity and the r_e–μ_e relation show a significant segregation of galaxies as a function of their concentration index (or, alternatively, their morphological type). In the case of the r_e-luminosity relation the difference in galaxy properties between low- and high-C_{31} galaxies is not extreme, and both classes of objects follow a well defined correlation, although with significantly different slopes and scatter (see the left panels in Fig. 8). The effect is more evident in the case of the r_e–μ_e correlation, as shown in the right panels of Fig. 8. It is clear from the figure that only for high C_{31} galaxies, irrespective of their morphological type, r_e and μ_e are correlated to produce the well known Kormendy relation of early-type galaxies. For low C_{31} galaxies, instead, no correlation is observed between the two parameters, except for a lack of objects with large r_e and very bright μ_e (the top left corner of the diagram). This result is in qualitative agreement with the finding of

[1] Although one must keep in mind that only two of the three parameters involved are statistically independent, as a result of our definition of effective radius and effective surface brightness: given the total flux f_t and the effective radius $r_e = r(f_t/2)$, we have $\mu_e = -2.5\log(f_t/2\pi r_e^2) + Z_p$.

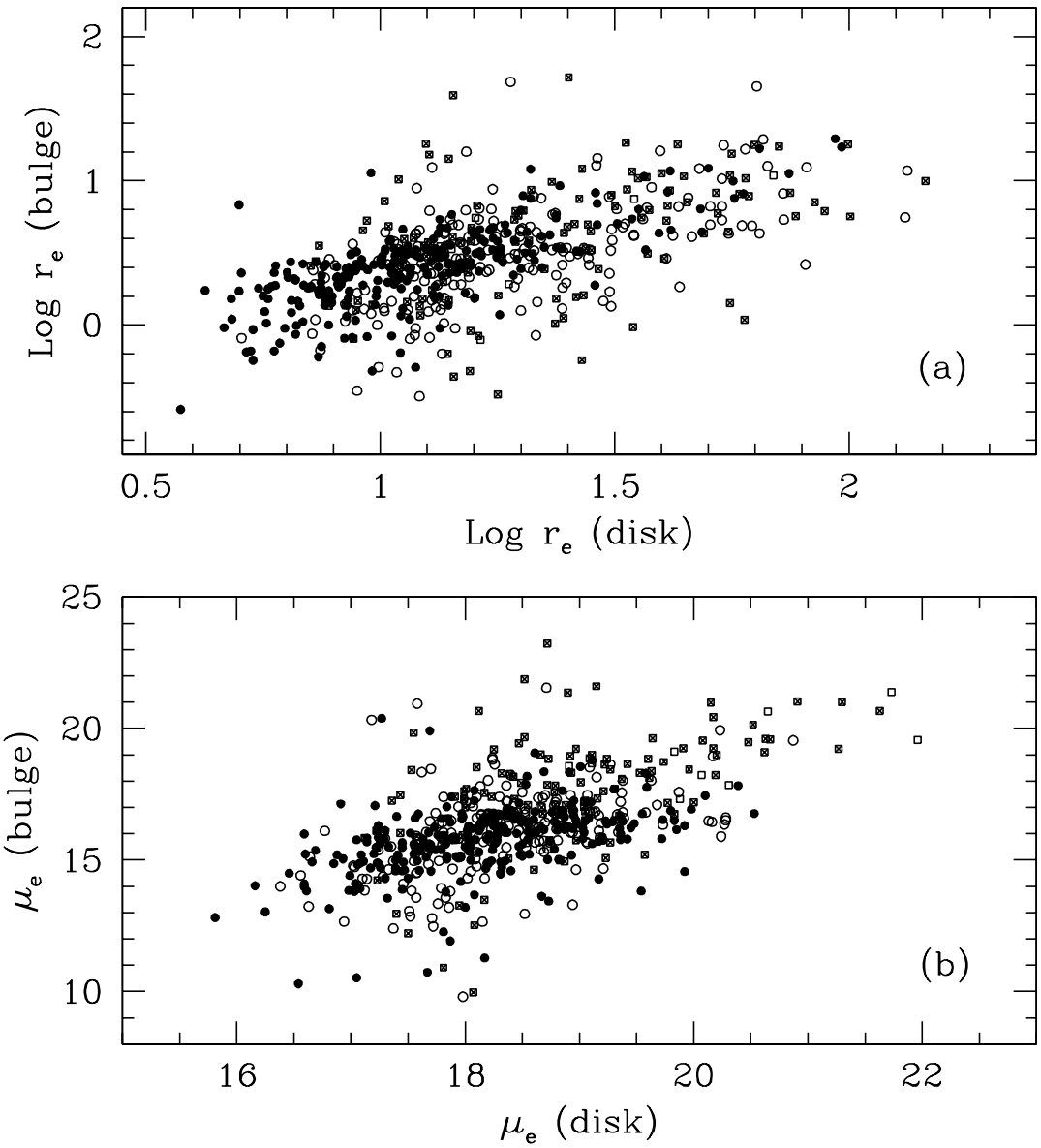

Fig. 9. The correlation between bulge and disk effective radius **a)** and between bulge and disk effective surface brightness **b)**. Plotting symbols are as in Fig. 3: filled circles represent E and S0 galaxies, empty circles Sa to Sb galaxies, crossed squares Sc to Sdm galaxies, open squares Im and BCD galaxies.

Graham & de Block (2001) that very late-type spirals (thus galaxies with low C_{31}) have smaller and fainter disks than earlier-type ones. The zone of avoidance at large r_e and very bright μ_e, which is common to galaxies of all C_{31} values, has been already discussed (for the case of disk galaxies only) by Dalcanton et al. (1997; see their Fig. 4), and has its origin in the existence of an exponential cut-off at the high-mass end of the mass function of galaxies (closely mirrored by the cutoff in the galaxy luminosity function).

6. Bulge and disk parameters

The main motivation for using a concentration index in our classification scheme instead of something like a bulge to disk light ratio was the fact that measurements of C_{31} do not require model-dependent decompositions of a galaxy light distribution, which carry with them systematic uncertainties very difficult to estimate. Still those decompositions are routinely carried out, and are used to analyze in fine detail models of galaxy formation. Courteau et al. (1996) were the first to report the existence of a correlation between disk and bulge scale lengths for two samples of late-type spirals, that they interpreted as evidence for the presence of secular evolution in driving bulge formation. Their result has been recently confirmed also by Khosroshahi et al. (2000). However these authors, as well as Graham & Prieto (1999), find systematic changes in the ratio of disk to bulge scale length as a function of morphological type, and they interpret this result as evidence against the formation of bulges via secular evolution of the disk of spiral galaxies.

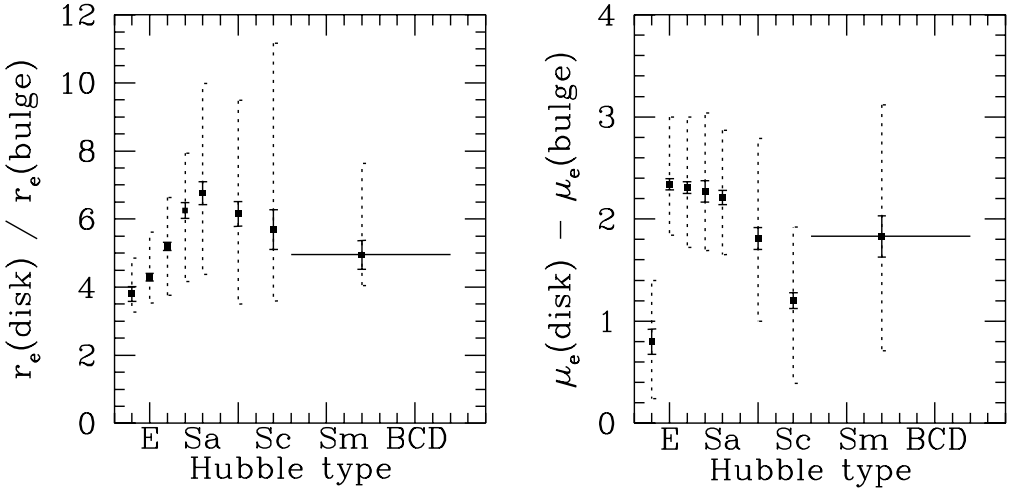

Fig. 10. The median of the ratio between disk and bulge effective radius **a)** and of the difference between disk and bulge effective surface brightness **b)** for different morphological types (filled squares), with the associated statistical uncertainty and the inter-quartile range of their value distribution (dased vertical lines). Types later than Sc are grouped together to improve statistics.

We have analyzed the relation between bulge and disk parameters for the 667 galaxies in our sample that required a bulge+disk decomposition of their surface brightness profile. We find that both the disk and bulge effective radius and disk and bulge effective surface brightness are correlated, although with a large scatter. These correlations are presented in Fig. 9, where different symbols identify galaxies of different morphological type (symbols are the same as in Figs. 3 and 6). There is also some marginal evidence for systematic changes with morphological type in the ratio between the two radii, or the difference between the two surface brightnesses, as shown in Fig. 10. In contrast with the finding of Graham & Prieto (1999), we find that Sa galaxies have a larger ratio between disk and bulge effective radius than later-type spirals, and they also have a much larger difference in effective surface brightness than later types. This difference cannot be considered really significant, as Graham & Prieto (1999) themselves have shown that a change in the function used to fit the surface brightness profile of the bulge (an exponential profile instead of a Sérsic one) leads to a complete reversal of their results, bringing them in agreement with ours. This same caveat applies to the comparison with the results obtained by Courteau et al. (1996): they used a fixed profile shape for fitting the bulge photometric profile, while we have chosen either a de Vaucouleurs $r^{1/4}$ or an exponential disk profile according to an objective χ^2 criterion. The large scatter which is superimposed on the correlations shown in Fig. 9 seems to argue against the presence of a single, homogeneous mechanism that could regulate the bulge formation and its interaction with the surrounding disk.

7. Discussion and conclusions

A classification scheme for any kind of object, either real or totally abstract ones, is really useful only if it can be used to sort properties of those objects other than those explicitly used for the classification itself. For example, the Harvard stellar spectra classification scheme, created purely on the basis of spectral shape and spectral line patterns, is still in use because it was later recognized that it sorts stars in terms of surface temperature, and ultimately in terms of mass. As far as galaxies are concerned, Hubble's tuning fork scheme is by far the most commonly use classification tool. The origin of its success, besides the fact that it is relatively easy to use, is mainly due to the fact that it helps sort important physical galaxy properties, like current stellar population and star formation history, or gas and dust content.

However this sorting is only a partial one, and while clear trends exist for many galaxy properties as a function of Hubble's type, it is also true that these properties show a large scatter within each type, so that there is a large overlap in their distribution between different types (see Roberts & Haynes 1994 for a recent review). We have shown two examples of this situation in Fig. 1. These large scatters naturally lead to the idea of including some new parameters in the classification scheme, to increase its discriminating power. However, other limitations within Hubble's scheme, namely its qualitative and quantized nature, and its failure to classify a significant fraction of known galaxies, severely limit the usefulness of any such extension. We have therefore decided to explore the possibility of replacing Hubble's scheme altogether. This is not a new idea, as complete replacements were already proposed in the past, most noticeably by Morgan (1958, 1959), Whitmore (1984), and most recently by BJC. Building on Whitmore's ideas, we have independently obtained a classification scheme that turns out to be qualitatively very similar to the one proposed by BJC, and is illustrated by Fig. 3.

Contrary to BJC, we do not make here any attempt at reproducing the sub-division among Hubble's types within

our scheme, as we are only interested in building a scheme that can give a complete description of galaxy properties based on a small number of quantitative and easy-to-measure parameters. In agreement with BJC we find that normal galaxies (we do not have peculiar, strongly interactive, or extremely low surface brightness galaxies in our sample) can be described by a three parameter model. Using Whitmore terminology, we can call these three parameters galaxy scale (for us the H-band luminosity), form (for us the concentration index C_{31}), and color (we use the $B-H$ color, but any optical or optical-near infrared color can be used for this purpose). The need for three parameters is clearly shown by objects that belong to the two different property regimes existing along the strongly non-linear relations between C_{31} and either color or luminosity. At low luminosity (see the bottom panels of Fig. 3) we need color information to distinguish between a dE and a dIrr galaxy with the same C_{31}, while at high luminosity we need C_{31} information to distinguish between an S0 and an Sc galaxy with the same color.

The three parameters are relatively easy to derive from photometric observation data, and do not require any modeling of the galaxy light distribution. However the measurement of C_{31} imposes constraints on the resolution of the imaging data that could be used to classify galaxies, and it is clear that even using our model it would be extremely difficult to rely on ground-based observations to classify high-redshift galaxies.

An alternative representation of the classification cube can be obtained substituting galaxy luminosity with effective surface brightness, taking advantage of the correlation existing between the two quantities (see Figs. 6 and 7). This is perhaps the most unexpected result of our analysis, as it is in contrast with previous results based on observations carried out at shorter wavelengths. We find that a single, well-defined relation exists between luminosity and $\mu_{\rm e}$ in the H-band, as opposed to the two separate regimes observed by Binggeli et al. (1984) in the B-band, and between $B-H$ or $B-V$ color and $\mu_{\rm e}$, as opposed to the much shallower relation between $B-V$ and $\mu_{\rm e}$ in the B-band presented by BJC. Actually, for $B-V<0.8$ the BJC relation is completely flat, as demonstrated by the vertical boundary between late- and intermediate-type galaxies in the upper panel of their Fig. 3, and as should be expected on the basis of Freeman's law (Freeman 1970). On the contrary, we find that surface brightness in the near-infrared is not a scale-free parameter, but it depends on the galaxy luminosity, confirming earlier results by Gavazzi et al. (1996c) and de Jong (1996).

These differences highlight the importance of selecting the "right" photometric band for mapping the structural properties of galaxies. In this respect near-infrared bands have two key advantages over optical ones: reduced dust extinction effects, and reduced effects of current star formation activity on both the galaxy total luminosity and surface brightness distribution. For these reasons, near-infrared luminosity traces quite accurately galaxy mass (see for example Gavazzi et al. 1996c, and Scodeggio et al. 1998). Using this luminosity-mass equivalence we can obtain an accurate picture of the role that galaxy mass has in determining the global structure of a galaxy, via the influence it has in determining the galaxy luminous matter mean density and global distribution.

If the observed correlation between mass and surface brightness is already an indication in favor of a scale-dependent galaxy collapse mechanism, the strong non-linearity of the relation between mass and concentration index C_{31} should pose very strong constraints on such a scenario. Strong light concentrations (high C_{31} values), that are somewhat correlated to the presence of a dominant spheroidal, bulge-like component (but not in a simple way, as the scatter in the C_{31}–B/T ratio seen in Fig. 2 demonstrates), appear only for luminous red galaxies, at $L_H > 10^{10}\ L_\odot$. Below that limit galaxies do not have enough mass to drive the concentration of mass and luminous matter towards their center. Above the limit this concentration is possible, but it does not take place automatically for all galaxies. If it happens, however, it must happen quite early during the evolution of a galaxy, or at least involve only old stellar populations without the onset of new star formation activity. In fact high values of C_{31} are present only among very red galaxies that must have formed a large fraction of their stars during the first few (one to three) billion years of their history.

This important role of galaxy mass in determining the galaxy structure matches a similar role that mass has in determining the star formation history of galaxies, at least for spiral ones (see Gavazzi & Scodeggio 1996 and also Boissier & Prantzos 2000). Unfortunately the link between galaxy mass and near-infrared luminosity is the only well established one along the path from a phenomenological classification scheme to a self consistent physical model, and we don't have other simple physical properties that can be unequivocally associated with star formation (i.e. color) and matter distribution within a galaxy, although it is obvious that angular momentum must be playing an important role in determining galaxy structure (see, for example, Dalcanton et al. 1997; Boissier & Prantzos 2000; Pierini et al. 2002). It is therefore not possible to build, based on the present data, a simple physical model that could be used, for example, to explore the origin of the scatter that is still present in all relations involving galaxy structural parameters.

References

Abraham, R. G., Valdes, F., Yee, H. K. C., & van den Bergh, S. 1994, ApJ, 432, 75

Arimoto, N., & Yoshii, Y. 1987, A&A, 173, 23

Bershady, M. A., Jangren, A., & Conselice, C. J. 2000, AJ, 119, 2645 (BJC)

Binggeli, B., Sandage, A., & Tarenghi, M. 1984, AJ, 89, 64

Binggeli, B., Sandage A., & Tammann G. A. 1985, AJ, 90, 1681

Boissier, S., & Prantzos, N. 2000, MNRAS, 312, 398

Boselli, A., Tuffs, R., Gavazzi, G., Hippelein, H., & Pierini, D. 1997, A&AS, 121, 507

Boselli, A., Gavazzi, G., Franzetti, P., Pierini, D., & Scodeggio, M. 2000, A&AS, 142, 73 (Paper IV)
Boselli, A., Gavazzi, G., Donas, J., & Scodeggio, M. 2001, AJ, 121, 753
Bower, R. G., Lucey, J. R., & Ellis, R. S. 1992, MNRAS, 254, 601
Burstein, D. 1979, ApJ, 234, 435
Courteau, S., de Jong, R. S., & Broeils, A. H. 1996, ApJ, 457, L73
Dalcanton, J. J., Spergel, D. N., & Summers, F. J. 1997, ApJ, 482, 659
de Carvalho, R. R., & Djorgovski, S. G. 1989, ApJ, 341, L37
de Jong, R. 1996, A&A, 313, 45
de Vaucouleurs, G. 1959, in Handbuch der Physik, Vol. 53, ed. S. Flugge (Berlin: Springer-Verlag), 275
de Vaucouleurs, G. 1977, in Evolution of Galaxies and Stellar Populations, ed. R. Larson, & B. Tinsley (New Haven: Yale University Observatory), 43
Djorgovski, S. G., & Davis, M. 1987, ApJ, 313, 59
Doi, M., Fukugita, M., & Okamura, S. 1993, MNRAS, 264, 832
Dressler, A., Lynden-Bell, D., Burstein, D., et al. 1987, ApJ, 313, 42
Faber, S. M., & Jackson, R. E. 1976, ApJ, 204, 668
Fish, R. A. 1964, ApJ, 139, 284
Freeman, K. C. 1970, ApJ, 160, 811
Gavazzi, G., & Scodeggio, M. 1996, A&A, 312, L29
Gavazzi, G., Pierini, D., Boselli, A., & Tuffs, R. 1996a, A&AS, 120, 489 (Paper I)
Gavazzi, G., Pierini, D., Baffa, C., et al. 1996b, A&AS, 120, 521 (Paper II)
Gavazzi, G., Pierini, D., & Boselli, A. 1996c, A&A, 312, 397
Gavazzi, G., Franzetti, P., Scodeggio, M., et al. 2000a, A&AS, 142, 65 (Paper III)
Gavazzi, G., Franzetti, P., Scodeggio, M., et al. 2000b, A&A, 361, 863, (Paper V)
Gavazzi, G., Zibetti, S., Boselli, A., et al. 2001, A&A, 372, 29 (Paper VII)
Gavazzi, G., Bonfanti, C., Boselli, A., & Scodeggio, M. 2002, ApJ, submitted
Graham, A. W., & Prieto, M. 1999, ApJ, 524, L23
Graham, A. W., & de Block, W. J. G. 2001, ApJ, 556, 177
Guzmán, R., Lucey, J. R., & Bower, R. G. 1993, MNRAS, 265, 731
Hubble, E. 1936, The Realm of the Nebulae (New Haven: Yale University Press)
Kennicutt, R. C. 1983, ApJ, 272, 54
Kent, S. M. 1985, ApJS, 59, 115
Khosroshahi, H. G., Wadadekar, Y., & Kembhavi, A. 2000, ApJ, 533, 162
Kormendy, J. 1977, ApJ, 218, 333
Morgan, W. W. 1958, PASP, 70, 364
Morgan, W. W. 1959, PASP, 71, 394
Okamura, S., Kodaira, K., & Watanabe, M. 1984, ApJ, 280, 7
Pierini, D., Gavazzi, G., Franzetti, P., Scodeggio, M., & Boselli, A. 2002, MNRAS, in press
Roberts, M., & Haynes, M. P. 1994, ARA&A, 32, 115
Sandage, A. 1961, The Hubble Atlas of Galaxies (Washington: Carnegie Insitute of Washington)
Sandage, A. 1986, A&A, 161, 89
Scodeggio, M., Giovanelli, R., & Haynes, M. 1997, AJ, 113, 2087
Scodeggio, M., Gavazzi, G., Belsole, E., Pierini, D., & Boselli, A. 1998, MNRAS, 301, 1001
Searle, L., Sargent, W. L. W., & Bagnuolo, W. G. 1973, ApJ, 179, 427
Sérsic, J. L. 1968, Atlas de Galaxias Australes (Cordoba: Observatorio Astronomico)
Tully, R. B., Mould, J. R., & Aaronson, M. 1982, ApJ, 257, 527
Visvanathan, N., & Sandage, A. 1977, ApJ, 216, 214
Whitmore, B. C. 1984, ApJ, 278, 61
Worthey, G. 1994, ApJS, 95, 107
Worthey, G., Trager, S. C., & Faber, S. M. 1996, in Fresh Views of Elliptical Galaxies, ASP Conf. Ser. 86, ed. A. Buzzoni, A. Renzini, & A. Serrano (San Francisco: ASP), 203
Zwicky, F., Herzog, E., Karpowicz, M., Kowal, C., & Wild, P. 1961–1968, Catalogue of Galaxies and Clusters of Galaxies, 6 vol. (Pasadena: California Institute of Technology)